Supplementary Materials and Methods

Human Stool Samples. Patients fulfilling the DSM IV criteria[1] for alcohol dependence and with active alcohol consumption were compared to a control group of non-alcoholic volunteers. Patient characteristics are shown in Supplemental Table 3. Fecal samples were either immediately frozen, or placed on ice and frozen within 2-5 hrs after the collection. Samples were kept frozen until they were processed. Written informed consent was obtained from all patients and healthy controls. The study protocol was approved by the Institutional Review Board from each institution involved.

16S rRNA and metagenomic sequencing. DNA from feces or intestinal contents from mice was extracted as previously described[2, 3]. Deep DNA pyrosequencing of the hypervariable V1–V3 region of prokaryotic 16S rRNA loci was performed to generate microbial community profiles using species-level (97% similarity) operational taxonomic unit-based classification and analysis as described in our previous publications[2, 3] except the YAP was used to orchestrate the workflow[4, 5]. Sequence reads are available under NCBI BioSamples SAMN02671702-SAMN02671718 under BioProject PRJNA89097.

For metagenomic sequence analysis, high molecular weight genomic DNA was extracted and purified from the ceca of alcohol and control animals as described[2]. Two bar-coded paired-end Illumina libraries were constructed from pooled DNA with an average insert size of 300 bp. Shotgun libraries were sequenced by 2x100bp paired-end sequencing using an Illumina HiSeq 2000 platform at a density of one library per lane, yielding 85,492,250 reads for the control and 75,238,322 reads for the alcohol treated group.

The Bowtie short read aligner was used to remove reads matching the MGSCv37/mm9 mouse genome assembly obtained from UCSC. Fragmented reads were removed using MateFilter.py, distributed within YAP (http://github.com/shpakoo/YAP). Reads were filtered so that 95% of bases

had a quality value of 30 or greater, using fastq_quality_filter and converted to FASTA format using fastq_to_fasta, both part of the FASTX-Toolkit (http://hannonlab.cshl.edu/fastx_toolkit/). Filtered sequences were assembled into contigs using the CLC Assembly Cell version 3.22.55708 using 30 CPUs and expecting paired ends to be 180–350 bp in length.

Contigs larger than 1000 bp in length were uploaded to the Metagenomics Analysis Server (MG-RAST) at metagenomics.anl.gov for annotation and metabolic reconstruction[6]. The MG-RAST KEGG Mapper was used under default settings to display differential abundances of enzymes involved in metabolism. Functional abundance of proteins was assessed by hierarchical classification using the KEGG Ortholog (KO) database with default settings. A table of KO abundance values was exported for the analysis of differences in normalized relative abundances of KO identifiers. Data can be accessed through MG-RAST.

Nucleotide sequences of the *fabD*, *fabF*, and *fabG* genes were pulled from all metagenomic contigs based on annotation from the JCVI metagenomics annotation pipeline and aligned separately using transAlign.pl[7]. The ends of the alignments were trimmed to conserved residues using belvu[8]. Based on the alignment, a bootstrapped Neighbor-joining tree was subsequently inferred using paupFasta, an in-house wrapper script (https://github.com/jhbadger/phyloFasta) for the PAUP* program[9]. The manipulation and drawing of phylogenetic trees was accomplished using the Interactive Tree Of Life (iTOL) web server[10] To determine average read depth, reads were first mapped to contigs containing *fab* genes using the CLC Workbench (http://www.clcbio.com/products/clc-genomics-workbench/) command line tool (clc-mapper, Version 4.21.104315) using default settings except similarity and length fraction which were set to 0.9 and 0.8, respectively. The sequence coverage of mapped reads was determined for each gene using BEDTools coverage (v2.20.1)[11].

Metabolomic analysis. Saturated short-chain fatty acids (SCFA), saturated medium-chain fatty acids (MCFA) and saturated long-chain fatty acids (LCFA) (C2:0–C18:0) concentrations in plasma and fecal samples were determined by solvent extraction followed by gas chromatography-mass spectrometry (GC-MS). Fecal samples were extracted in a solvent containing ^{13}C-labeled internal standards (D7-butyric acid and D11-hexanoic acid). Samples were homogenized using a probe sonicator and centrifuged; supernatants were transferred to a new Eppendorf tube. After layers separated, bottom layers were transferred to autosampler vials for GC-MS analysis. Internal standards and external calibration curves were used to calculate the concentrations in the samples. Absolute quantities of free fatty acids were normalized to the sample mass.

Real-time qPCR. RNA was extracted from mouse tissues and cDNAs were generated[12]. Primer sequences for mouse genes were obtained from the NIH qPrimerDepot. To quantify the total bacterial load present in the cecum, the qPCR value of 16S rRNA gene for each sample was multiplied by the total amount of DNA/g of cecal content. The following published bacterial primer sequences were used: 16S rRNA gene[13], *Lactobacillus* species[14], *Lactobacillus rhamnosus*[15], *Akkermansia muciniphila*[16], *Prevotella*[17], *Enterococcus faecalis* and *Clostridium cluster XI*[18], *Firmicutes*[19], and *Bacteroidetes*[20].

The genomic sequences of the *fabD*, *fabF*, and *fabG* from bacteria were obtained via metagenomic sequencing analysis. After alignment, consensus sequences at noise threshold (20%) and maximum threshold (70%–80%) were obtained and used for degenerate primer design, by primer premier 5.0 software. The primer sequences are as follows: *fabG* forward: 5’-GGMAATGCHGGWCARRCIAA-3’; *fabG* reverse: 5’-GTCATRTCWGTHTCDATIAA-3’; *fabF* forward: 5’-GAYGCWTAYCAYATGACA-3’; *fabF* reverse:

5’-GATGTDCCRTGWRCRTTGAT-3’; *fabD* forward: 5’-GTIGYTSCHGCMAAYTAIAA-3’; *fabD* reverse: 5’-GGICCRAKYTCWAYIAA-3’. Genomic *fabD*, *fabF* and *fabG* expression was normalized to 16S rRNA. PCR products from both mouse and human samples were sequenced to confirm correct amplification.

For bacterial RNA extraction, bacteria were harvested using stop solution (95% Ethanol, 5% TRIzol (Life Technologies)). Cells were then centrifuged at 10,000rpm at 4℃ for 10 minutes. After centrifugation, the supernatant was decanted and cell pellets were frozen at -80℃ until use. Total RNA was isolated using 2 methods: (1) Nucleospin RNA XS columns with the following changes. Cell pellets were resuspended in 100µl TE buffer (10mM Tris-HCl, 1mM EDTA; pH8) with 23,000U Ready-lyse Lysozyme Solution (Epicentre), 1 µl Proteinase K Solution (20 mg/ml, Life Technologies), and 20 U SUPERase-In (Life Technologies) and incubated at 37℃ for 15 minutes. After incubation, 100µl Buffer RA1 and 2µl TCEP were added to the sample and then vigorously vortexed. Turbidity and viscosity were reduced by filtering the sample through the violet-ringed Nucleospin Filters included in the kit using centrifugation. 100µl of 70% ethanol was added to the lysate, and the sample was loaded onto the NucleoSpin RNA XS column. From this point, the standard protocol was followed beginning at step 6. Purified RNA was eluted with RNase free H_20. (2) Cell pellets were resuspended and incubated with Lysozyme Solution, Proteinase K and SUPERase-In as described above. Then RNA was extracted according to TRIzol protocol. Finally, DNA was purified and digested using Nucleospin RNA XS columns following the manufacturer’s instructions. After RNA isolation, reverse transcription (Life Technologies) was performed using random primers. cDNA was amplified using *fab* primer sequences as above.

Mouse gene expression and amplification of genomic bacterial DNA and cDNA were determined with Sybr Green, using the ABI StepOnePlus real-time PCR system.

Plasma assays. Plasma levels of ethanol were measured using the Ethanol Assay Kit (BioVision). Levels of ALT were measured using Infinity ALT kit (Thermo Scientific). Endotoxin measurement was described previously[21].

TBARS assay. Hepatic lipid peroxidation was quantified by TBARS formation using the Oxiselect TBARS Assay Kit (Cell Biolabs).

Triglyceride measurement. Hepatic triglyceride levels were measured using the Triglyceride Liquid Reagents Kit (Pointe Scientific). For fecal triglyceride measurement, stool samples were mixed with phosphate-buffered saline and centrifuged, to separate solid particles. Triglyceride concentrations in supernatants were determined.

Bacterial cultures. For ethanol treated experiment, *Lactobacillus rhamnosus* GG (ATCC 53103) was cultured in MRS broth (Difco). For fatty acid treated experiment, *Lactobacillus rhamnosus* GG was cultured in modified MRS broth (MRS(-)): 10.0 g peptone, 6.0 g beef extract, 4.0 g yeast extract, 20.0 g dextrose, 2.0 g K_2HPO_4, 0.2 g $MgSO_4 \cdot 7H_2O$, 40 mg $MnSO_4 \cdot H_2O$, 2.0 g ammonium citrate dibasic, 5.0 g $NaOAc \cdot 3H_2O$ in 1L H_2O. Fatty acids were dissolved in 0.1 M NaOH to 10 mM as stock and supplemented to MRS(-) broth. Bacteria were incubated anaerobically at 37°C for 24 or 48 hrs. Bacterial growth was determined by measuring the OD_{600} value from each individual sample. For Caco-2 experiments, *Lactobacillus rhamnosus* GG was cultured in MRS broth (Difco) until OD_{600} reached 0.6, the supernatant was collected after centrifugation and stored at –80℃ until analysis. For *ex vivo* microbiome analysis, cecum contents were harvested from control mice and inoculated in modified PETC medium[22] (Yeast extract and all other carbon sources were removed to make ethanol the only carbon source instead) under anaerobic conditions. Genomic DNA was extracted from bacteria prior to incubation with

ethanol (Pre-EtOH group) or following ethanol (1:1000 v/v) treatment (Post-EtOH group) for 9 days.

Staining procedures. Formalin-fixed tissue samples were embedded in paraffin and stained with hematoxylin-eosin (Surgipath), or with 4-hydroxynonenal (HNE; Alpha Diagnostic Intl. Inc.) using standard staining protocols. To assess apoptosis, paraffin-embedded intestinal sections were stained using the TUNEL kit from Roche. Frozen sections (5μm) were used for Oil Red O staining. For immunofluorescence of intestinal tight junction proteins, frozen intestinal sections were stained using anti-occludin and anti–claudin-2 antibodies and a fluorescein isothiocyanate–conjugated secondary antibody (all Invitrogen) as described[12]. Nuclei were stained with Hoechst (blue). Control sections were stained with an isotype antibody instead of the primary antibody and showed no staining. To detect TNFα producing monocytes and macrophages, tissue was stained with primary antibodies against Lys6C (Abcam), F4/80 (eBioscience) and TNFα (Abcam) and positive reactions were visualized using fluorescent labeled secondary antibodies. 5-6 random high power fields per slide were chosen for analysis, and double positive cells were expressed as percentage of F4/80 or Lys6C positive cells in the lamina propria. Nuclei are stained with DAPI (blue).

Immunoblot analyses. All materials used to measure *E. coli* proteins in the liver were sterile and pyrogen free. To measure expression of CYP2E1, mouse liver microsomes were isolated as described[21]. Immunoblot analysis was performed using anti-CYP2E1 (Millipore Corporation), anti-occludin (Invitrogen), anti-claudin-2 (Invitrogen), and anti-*E. coli* (DAKO) antibodies. Anti-VDAC1 (Abcam) was used to ensure equal loading for microsomal extracts; anti-β-actin (Sigma-Aldrich) or anti-tubulin (Santa Cruz) antibodies were used as loading controls for hepatic and intestinal samples, respectively. Immunoblots were analyzed by densitometry, using NIH Image J.

Caco-2 monolayer cell culture. Caco-2 cells (ATCC HTB-37) were cultured in Dulbecco's Modified Eagle Medium (DMEM) supplemented with 100 U/ml penicillin, 100 µg/ml streptomycin, 15 mM HEPES, and 10% fetal bovine serum, at 37℃ in a 5% CO_2 environment. Caco-2 cells were subcultured after digestion with 0.25% trypsin-EDTA and passages 19–21 were used. Cells were grown on Transwell inserts (Costar, Corning) for 14-18 days to polarize and differentiate into epithelium cell-like monolayer. Polarized cell monolayers were starved of serum overnight; fatty acid mixed with bovine serum albumin[23] was added into the medium at indicated concentrations for 4 hrs. Cells were then incubated with acetaldehyde as previously described[24]. After 4 hrs acetaldehyde exposure, TEER was measured by Evom epithelial voltohmmeter (World Precision Instruments). For the *Lactobacillus rhamnosus* GG supernatant experiment, DMEM was supplemented with bacterial culture supernatants at 1% concentration; TEER was measured 4.5 hrs after acetaldehyde exposure.

Stable Isotope Probe DNA Analysis. Mice were gavaged with ^{13}C-labeled palmitic acid (Cambridge Isotope Laboratories; 66 mg/kg dissolved in sunflower seed oil) once daily for 3 consecutive days. Control mice received unlabeled palmitic acid (Sigma) at the same dose. A total of 10 µg DNA extracted from cecal contents was dissolved in gradient buffer (0.1 M Tris, 0.1 M KCl and 1 mM EDTA)[25] and CsCl was added at the final concentration of 1 g/ml. Ethidium bromide (1mg) was added to the DNA solution and transferred to polyallomer ultracentrifugation tubes (13–51 mm; Beckman). Following ultracentrifugation (50,000 rpm, 24 hrs, 20℃, SW 5 5 Ti rotor), active-heavy (^{13}C) and inactive-light (^{12}C) DNA were visible under UV light and extracted. After fractionation, DNA from the unlabeled palmitic acid (control) and ^{13}C-labeled palmitic acid group was collected at active-heavy (^{13}C) position. DNA was precipitated, dissolved in dH_20 (10 ng/µl) and used for qPCR

amplification. Amplification results were normalized to 16S rRNA in each group. *E. coli* incubated with ^{13}C-labeled glucose or unlabeled glucose were used as positive controls (Supplemental Figure 16).

Statistics. Results are expressed as mean±SEM. Significance was evaluated using the unpaired Student *t* test. Correlation coefficients were calculated by Spearman's rank correlation method in human samples. A *p*-value less than 0.05 was considered to be a statistically significant difference.

Supplemental Figure Legends

Supplemental Figure 1. Daily saturated fatty acid and unsaturated fatty acid pellet consumption. C57BL/6 mice were fed saturated fatty acids (SF) or unsaturated fatty acids (USF) and received intragastric isocaloric (n=3) or ethanol-containing (n=6-7) diets for 3 weeks.

Supplemental Figure 2. Ethanol reduces the abundance of bacterial fatty acid biosynthetic genes. Cecal contents from control mice were incubated under anaerobic conditions in modified PETC medium with ethanol. Prior (Pre-EtOH) and following incubation with EtOH for 9 days (Post-EtOH), genomic DNA was extracted from cecal contents. (A) qPCR analysis for bacterial *fabF*, *fabG* and *fabD* genomic DNA was performed (n = 4-5). (B) Bacterial mRNA level of *fabF* (n = 10), *fabG* (n = 10) and *fabD* (n = 5). (C) C57BL/6 mice were fed intragastric isocaloric (control) (n=3) or ethanol-containing diets (n=3) for 3 weeks. Consensus neighbor-joining trees are depicted using multiple alignments of *fabF*, *fabD*, and *fabG* genes from assembled metagenomic sequences. The gray circles along the branches denote percent occurrence of nodes among 100 bootstrap replicates greater than 80. Yellow-highlighted regions denote regions of the tree lacking alleles from alcohol-fed mice. The circles illustrate average read coverage of genes from terminal branches where alcohol and control groups share a common

node. The numbers indicate the average read depth. The scale bar represents the number of nucleotide substitutions. *p<0.05.

Supplemental Figure 3. Measurement of saturated fatty acids in intestines of mice. C57BL/6 mice were fed intragastric isocaloric (control) (n=3) or ethanol-containing diets (n=7) for 3 weeks. SCFA, MCFA, and LCFA in cecal contents. N.D.: non-detected. *p<0.05.

Supplemental Figure 4. Alcohol feeding does not affect fatty acid synthesis gene expression in the host. C57BL/6 mice were fed intragastric isocaloric (n=4) or ethanol-containing (n=3) diets for 3 weeks. (A - D) qPCR to measure levels of *Srebp1*, *Fasn*, *Acc1*, and *Scd1* mRNAs in intestinal segments. *p<0.05.

Supplemental Figure 5. Ratios of liver:body weight in mice. C57BL/6 mice were fed saturated fatty acids (SF) or unsaturated fatty acids (USF) and received intragastric isocaloric (n=3) or ethanol-containing (n=7) diets for 3 weeks. Liver weight is shown as a percentage of body weight.

Supplemental Figure 6. Saturated fatty acid feeding decreases hepatic chemokine expression. C57BL/6 mice were fed saturated fatty acids (SF) or unsaturated fatty acids (USF) and received intragastric isocaloric (n=3) or ethanol-containing (n=7) diets for 3 weeks. Hepatic *Ccl2* (A), *Ccl3* (B) and *Cxcl2* (C) gene expression was determined. *p<0.05.

Supplemental Figure 7. Triglyceride content in feces. C57BL/6 mice were fed saturated fatty acids (SF) or unsaturated fatty acids (USF) and received intragastric ethanol-containing (n=4) diets for 3 weeks. Feces were collected and total triglycerides (TG) were measured.

Supplemental Figure 8. Saturated fatty acid feeding increases intestinal levels of saturated fatty acids. C57BL/6 mice were fed saturated fatty acids (SF) or unsaturated fatty acids (USF) and received intragastric isocaloric (n=3) or alcohol (n=7) diets for 3 weeks. C16:0 (A) and C18:0 (B) levels in the cecum. *p<0.05.

Supplemental Figure 9. Plasma long-chain fatty acid concentration. C57BL/6 mice were fed saturated fatty acids (SF) or unsaturated fatty acids (USF) and received an intragastric ethanol-containing diet for 3 weeks. Pooled plasma samples from 7 mice in each group were analyzed for total C16:0 and C18:0.

Supplemental Figure 10. Saturated fatty acid feeding does not affect alcohol absorption and metabolism. C57BL/6 mice were fed saturated fatty acids (SF) or unsaturated fatty acids (USF) and received intragastric isocaloric (n=3) or alcohol (n=7) diets for 3 weeks. (A) Levels of ethanol in plasma. (B) Hepatic levels of *Adh1* mRNA. (C) Immunoblot for CYP2E1 protein in liver microsomes; VDAC1 is shown as the loading control for liver microsomes.

Supplemental Figure 11. Saturated fatty acid feeding reduces plasma endotoxin levels after chronic alcohol feeding. C57BL/6 mice were fed saturated fatty acids (SF) or unsaturated fatty acids (USF) and received intragastric alcohol (n=7) diets for 3 weeks. Plasma LPS levels were measured. *p<0.05.

Supplemental Figure 12. Intestinal apoptosis and morphology following saturated fatty acid supplementation. C57BL/6 mice were fed saturated fatty acids (SF) or unsaturated fatty acids (USF) and received intragastric isocaloric (n=3) or ethanol-containing (n=5-7) diets for 3 weeks. (A) TUNEL staining and (B) H&E staining of ileal sections.

Supplemental Figure 13. Saturated fatty acid feeding reduces intestinal inflammation after chronic alcohol administration. C57BL/6 mice were fed saturated fatty acids (SF) or unsaturated fatty acids (USF) and received intragastric alcohol (n=7) diets for 3 weeks. (A and B) *Ccl2* mRNA (A) and *TNFα* mRNA (B) levels in the ileum. (C-F) Ileal sections were stained with Lys6C or F4/80 (red) and TNFα (green) by immunofluorescence. Nuclei are stained in blue. (C and E) Representative intestinal sections are shown. (D and F) Quantification of Lys6c/TNFα and F4/80/TNFα double positive cells. *p<0.05.

Supplemental Figure 14. Saturated fatty acids do not protect monolayers of Caco-2 cells from disruption by acetaldehyde. Caco-2 cells were grown on transwell inserts for 14–18 days and allowed to differentiate into monolayers; they were then incubated with acetaldehyde in the presence of saturated fatty acids palmitic acid (A) and stearic acid (B) or unsaturated oleic acid (C) and linoleic acid (D) (n=3). TEER values were measured. *p<0.05.

Supplemental Figure 15. 16S rRNA gene sequences. C57BL/6 mice were fed saturated fatty acids (SF) or unsaturated fatty acids (USF) and received intragastric isocaloric (n=2-3) or ethanol-containing (n=6) diets for 3 weeks. Cecum samples were collected and 16S rRNA genes were sequenced using 454 Titanium technology. The graph demonstrates the percentages of each genus.

Supplemental Figure 16. Image of ^{12}C- and ^{13}C-containing DNA after ultracentrifugation. Left: *E. coli* was cultured with ^{13}C-labeled glucose overnight, genomic DNA was extracted and ^{12}C-containing DNA was separated from ^{13}C-containing DNA by CsCl density gradient ultracentrifugation. Right: Mice were gavaged with ^{13}C-labeled palmitic acid

daily for 3 days, cecum content DNA was extracted and separated by ultracentrifugation. ^{12}C- and ^{13}C-DNA was then collected from the same position shown in the left panel.

References

1. Ball SA, Tennen H, Poling JC, Kranzler HR, Rounsaville BJ. Personality, temperament, and character dimensions and the DSM-IV personality disorders in substance abusers. J Abnorm Psychol 1997;106:545-53.
2. Yan AW, Fouts DE, Brandl J, Starkel P, Torralba M, Schott E, et al. Enteric dysbiosis associated with a mouse model of alcoholic liver disease. Hepatology 2011;53:96-105.
3. Fouts DE, Torralba M, Nelson KE, Brenner DA, Schnabl B. Bacterial translocation and changes in the intestinal microbiome in mouse models of liver disease. J Hepatol 2012;56:1283-92.
4. **Fouts DE, Szpakowski S,** Purushe J, Torralba M, Waterman RC, MacNeil MD, et al. Next generation sequencing to define prokaryotic and fungal diversity in the bovine rumen. PLoS One 2012;7:e48289.
5. Fouts DE, Pieper R, Szpakowski S, Pohl H, Knoblach S, Suh MJ, et al. Integrated next-generation sequencing of 16S rDNA and metaproteomics differentiate the healthy urine microbiome from asymptomatic bacteriuria in neuropathic bladder associated with spinal cord injury. J Transl Med 2012;10:174.
6. Meyer F, Paarmann D, D'Souza M, Olson R, Glass EM, Kubal M, et al. The metagenomics RAST server - a public resource for the automatic phylogenetic and functional analysis of metagenomes. BMC Bioinformatics 2008;9:386.
7. Wong C, Yarbrough GG. Effects of the diethyl and dimethyl esters of glutamic acid on morphine anti-nociception in the rat. Can J Physiol Pharmacol 1975;53:509-12.

8. Hiklova-Sera D, Sery Z, Gazarek F, Vojacek K, Rocek V, Valach V. [Our experience with the treatment of a pathological secretion of the female mammary gland (author's transl)]. Cesk Gynekol 1975;40:23-7.

9. Wilgenbusch JC, Swofford D. Inferring evolutionary trees with PAUP*. Curr Protoc Bioinformatics 2003;Chapter 6:Unit 6 4.

10. Letunic I, Bork P. Interactive Tree Of Life (iTOL): an online tool for phylogenetic tree display and annotation. Bioinformatics 2007;23:127-8.

11. Fryer MW, Gage PW, Neering IR, Dulhunty AF, Lamb GD. Paralysis of skeletal muscle by butanedione monoxime, a chemical phosphatase. Pflugers Arch 1988;411:76-9.

12. Hartmann P, Haimerl M, Mazagova M, Brenner DA, Schnabl B. Toll-like receptor 2-mediated intestinal injury and enteric tumor necrosis factor receptor I contribute to liver fibrosis in mice. Gastroenterology 2012;143:1330-1340 e1.

13. Maeda H, Fujimoto C, Haruki Y, Maeda T, Kokeguchi S, Petelin M, et al. Quantitative real-time PCR using TaqMan and SYBR Green for *Actinobacillus actinomycetemcomitans*, *Porphyromonas gingivalis*, *Prevotella intermedia*, *tetQ* gene and total bacteria. FEMS Immunol Med Microbiol 2003;39:81-6.

14. **O'Shea CJ, McAlpine P,** Sweeney T, Varley PF, O'Doherty JV. Effect of the interaction of seaweed extracts containing laminarin and fucoidan with zinc oxide on the growth performance, digestibility and faecal characteristics of growing piglets. Br J Nutr 2014;111:798-807.

15. Alander M, Satokari R, Korpela R, Saxelin M, Vilpponen-Salmela T, Mattila-Sandholm T, et al. Persistence of colonization of human colonic mucosa by a probiotic strain, *Lactobacillus rhamnosus* GG, after oral consumption. Appl Environ Microbiol 1999;65:351-4.

16. Bergstrom A, Licht TR, Wilcks A, Andersen JB, Schmidt LR, Gronlund HA, et al. Introducing GUt low-density array (GULDA): a validated approach for qPCR-based intestinal microbial community analysis.

FEMS Microbiol Lett 2012;337:38-47.

17. Kumagai H, Maisawa S, Tanaka M, Takahashi M, Takasago Y, Nishijima A, et al. Intestinal microbiota and secretory immunoglobulin A in feces of exclusively breast-fed infants with blood-streaked stools. Microbiol Immunol 2012;56:657-63.
18. Lu H, Wu Z, Xu W, Yang J, Chen Y, Li L. Intestinal microbiota was assessed in cirrhotic patients with hepatitis B virus infection. Intestinal microbiota of HBV cirrhotic patients. Microb Ecol 2011;61:693-703.
19. Guo X, Xia X, Tang R, Zhou J, Zhao H, Wang K. Development of a real-time PCR method for *Firmicutes* and *Bacteroidetes* in faeces and its application to quantify intestinal population of obese and lean pigs. Lett Appl Microbiol 2008;47:367-73.
20. **Nakanishi Y, Murashima K,** Ohara H, Suzuki T, Hayashi H, Sakamoto M, et al. Increase in terminal restriction fragments of *Bacteroidetes*-derived 16S rRNA genes after administration of short-chain fructooligosaccharides. Appl Environ Microbiol 2006;72:6271-6.
21. Hartmann P, Chen P, Wang HJ, Wang L, McCole DF, Brandl K, et al. Deficiency of intestinal mucin-2 ameliorates experimental alcoholic liver disease in mice. Hepatology 2013;58:108-19.
22. Nagarajan H, Sahin M, Nogales J, Latif H, Lovley DR, Ebrahim A, et al. Characterizing acetogenic metabolism using a genome-scale metabolic reconstruction of Clostridium ljungdahlii. Microb Cell Fact 2013;12:118.
23. Cousin SP, Hugl SR, Wrede CE, Kajio H, Myers MG, Jr., Rhodes CJ. Free fatty acid-induced inhibition of glucose and insulin-like growth factor I-induced deoxyribonucleic acid synthesis in the pancreatic beta-cell line INS-1. Endocrinology 2001;142:229-40.
24. Rao RK. Acetaldehyde-induced barrier disruption and paracellular permeability in Caco-2 cell monolayer. Methods Mol Biol 2008;447:171-83.

25. Dunford EA, Neufeld JD. DNA stable-isotope probing (DNA-SIP). J Vis Exp 2010;42:e2027.

Author names in bold designate shared co-first authors

Supplemental Table 1

Fatty Acid Composition of Corn Oil

Fatty acid	Percentage (%)
C14:0	Trace
C16:0	10.8
C16:1	Trace
C18:0	2.1
C18:1	26.5
C18:2	60.0
C18:3	0.6

Supplemental Table 2

Fatty Acid Composition of 80-S Hydrogenated Soya Glyceride

Fatty acid	Percentage (%)
C16:0	12
C18:0	85
C18:1	3

Supplemental Table 3

Subject Characteristics

Subjects	Sex	Age	Race*	BMI	Alcoholic liver disease
Controls	M	20	C	26	
	M	25	AA	28	
	M	31	AA	26	
	M	43	C	29	
	F	51	AA	36	
	M	61	C	29	
Active Alcoholics	M	40	AA	23	no ALD
	M	40	AA	24	no ALD
	M	46	C	18	no ALD
	M	48	AA	26	no ALD
	F	53	AA	28	no ALD
	M	55	C	23	no ALD
	M	53	C	31	no ALD
	F	52	C	34	no ALD
	M	55	C	31	no ALD
	M	71	C	34	no ALD
	F	39	C	36	no ALD
	M	56	AA	33	AST 42, ALT 73
	F	54	C	23	Child A cirrhosis
	M	59	C	30	Child A cirrhosis
	M	28	C	31	Child C cirrhosis
	M	49	C	23	Child C cirrhosis

*C=Caucasian, AA=African American

Supplemental Figure 1

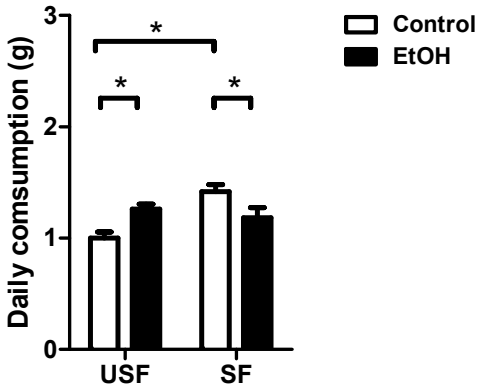

Supplemental Figure 2 Continued

C

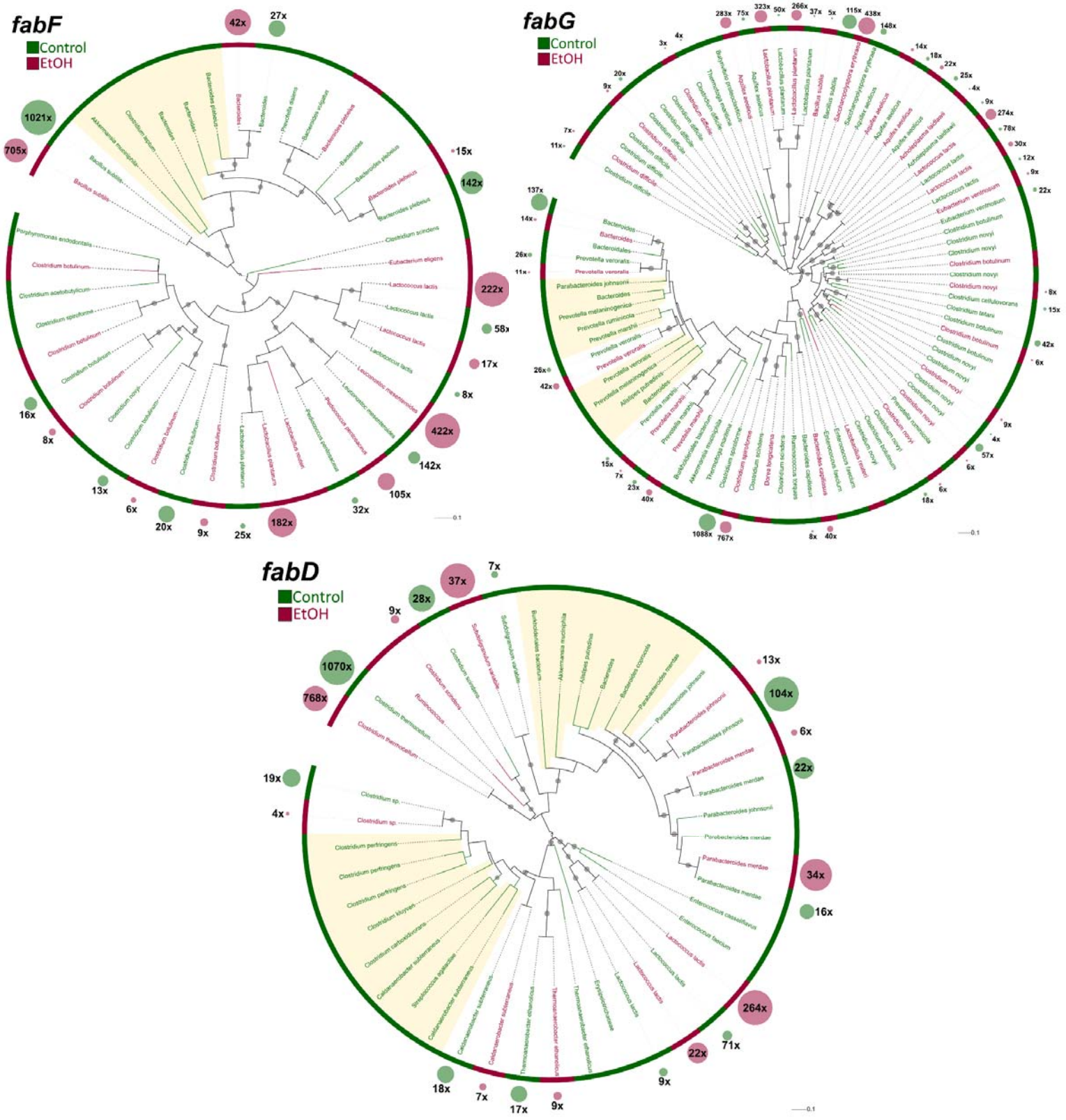

Supplemental Figure 2

A

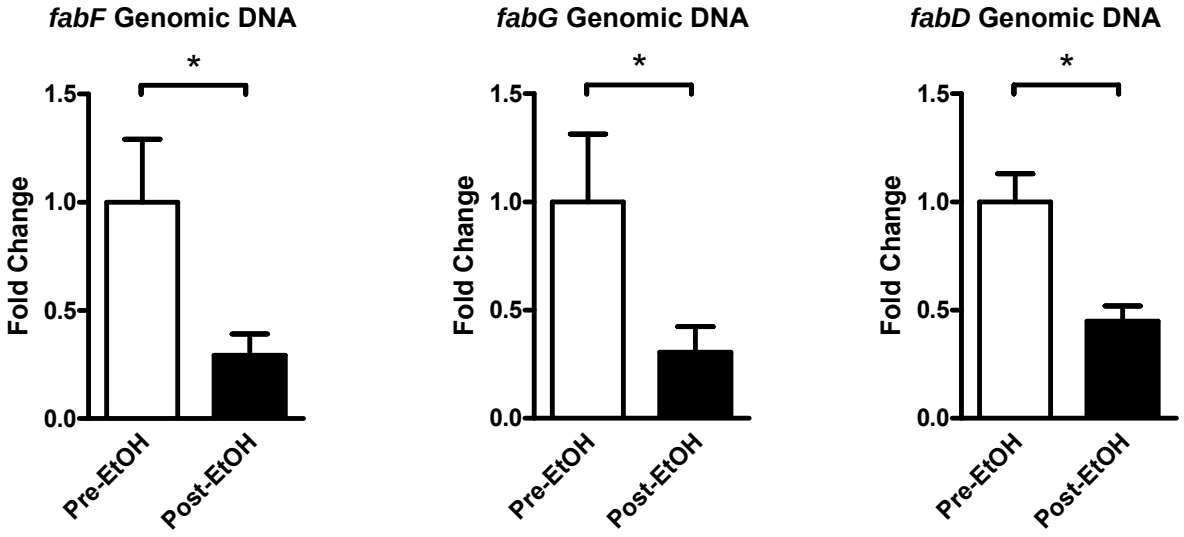

B

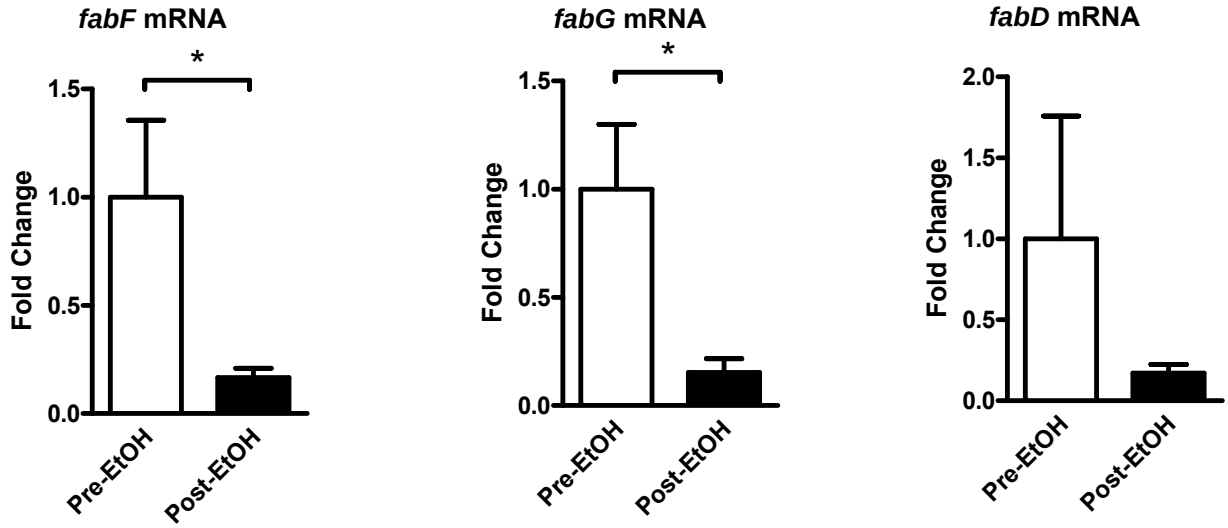

Supplemental Figure 3

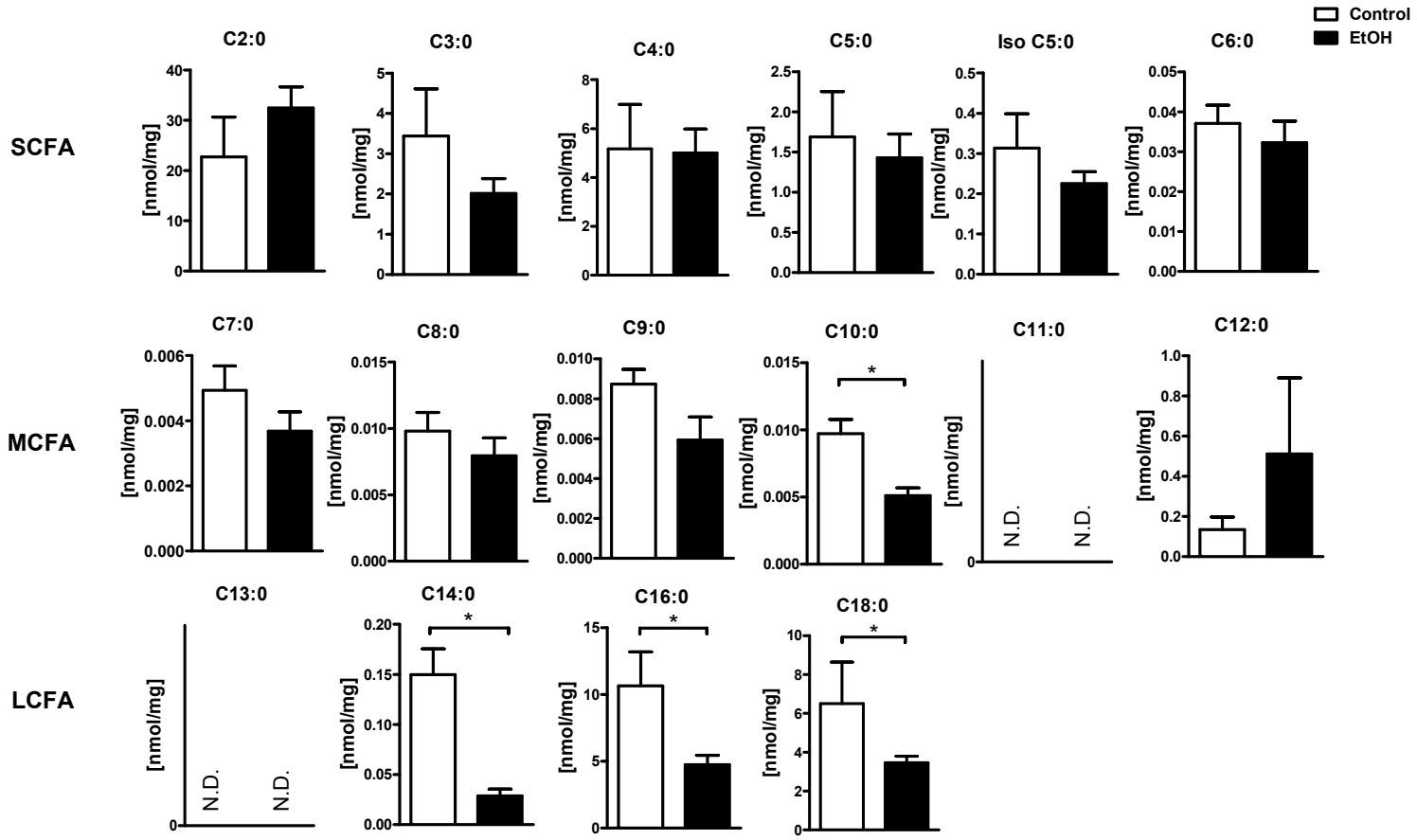

Supplemental Figure 4

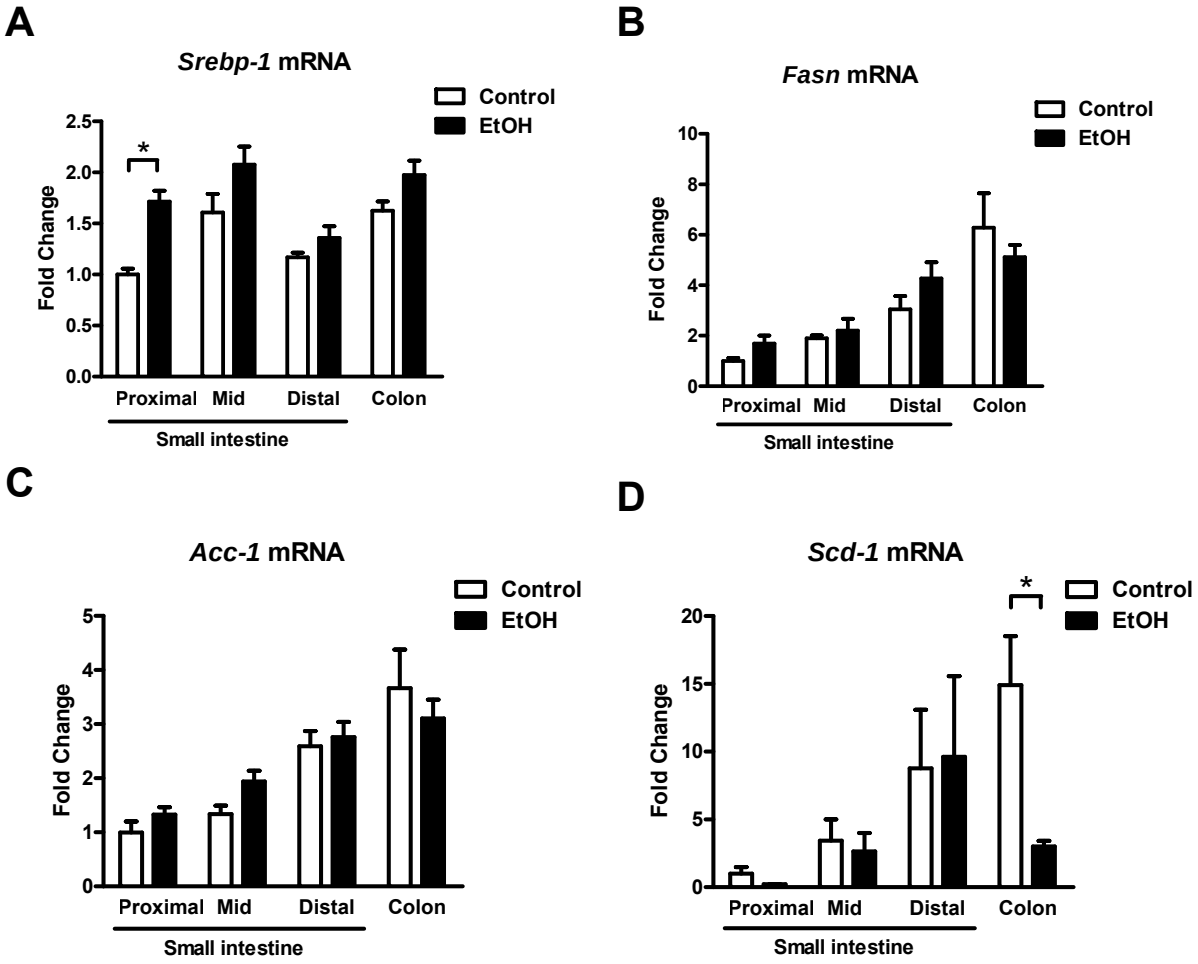

Supplemental Figure 5

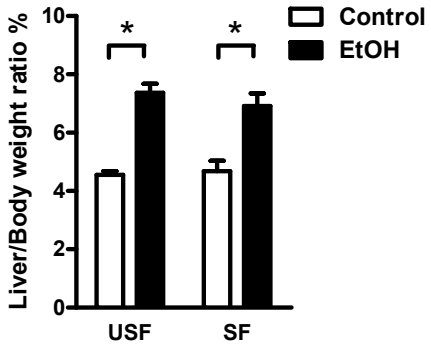

Supplemental Figure 6

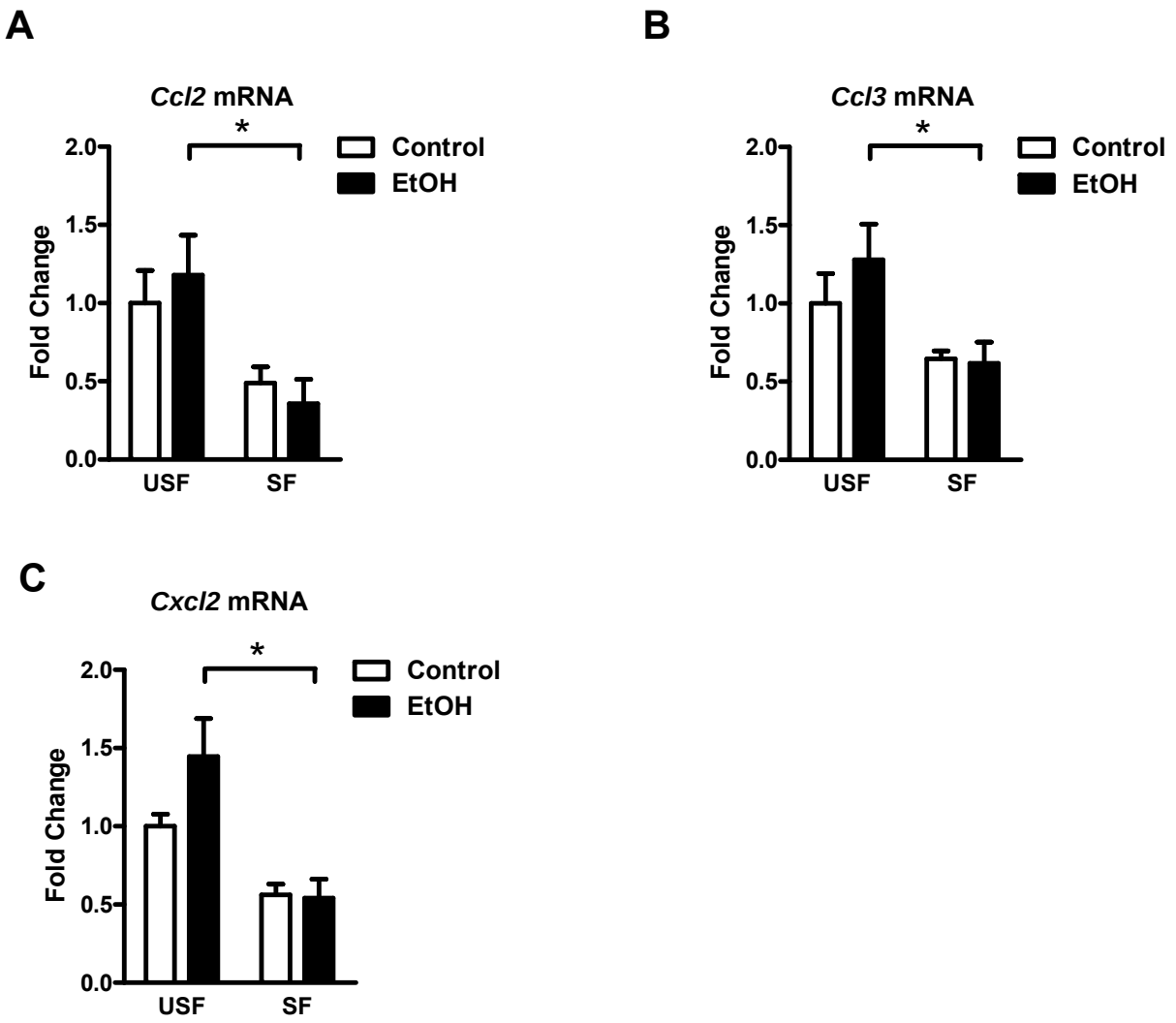

Supplemental Figure 7

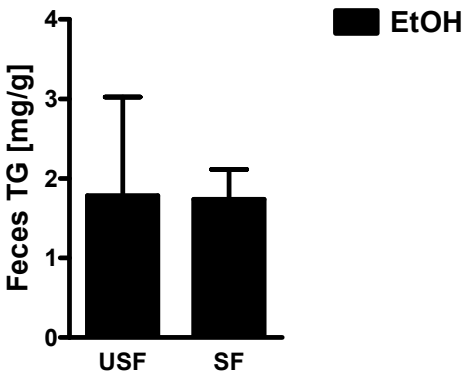

Supplemental Figure 8

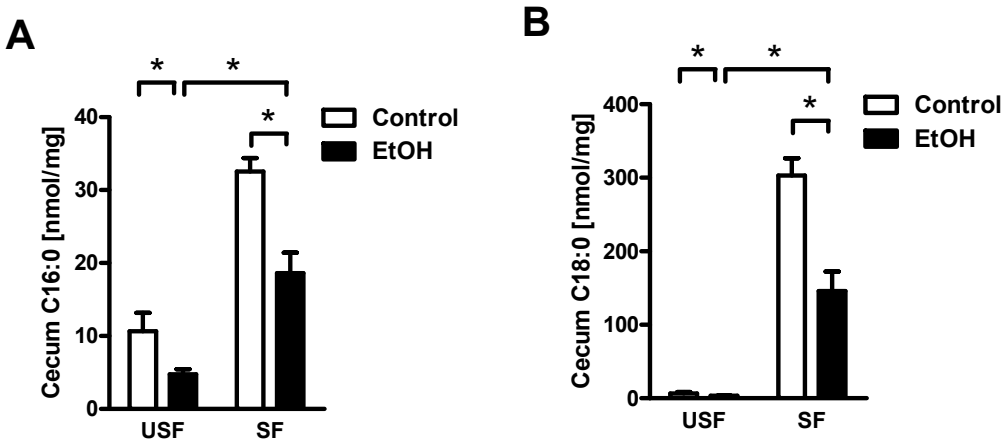

Supplemental Figure 9

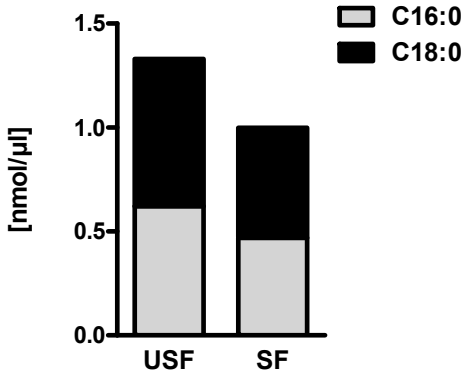

Supplemental Figure 10

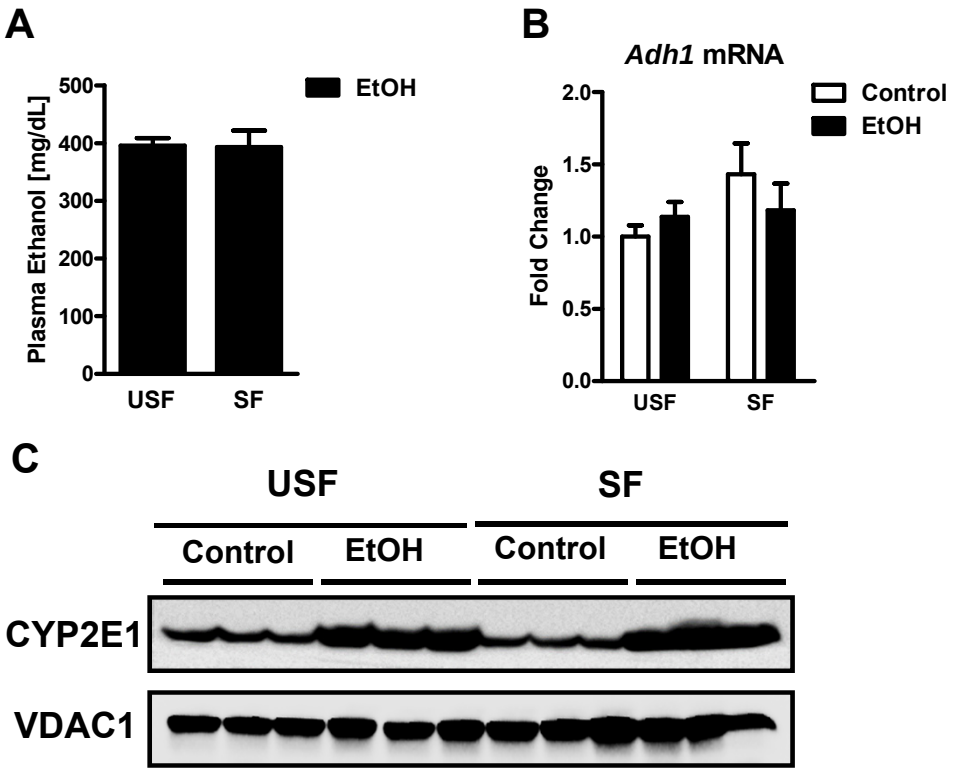

Supplemental Figure 11

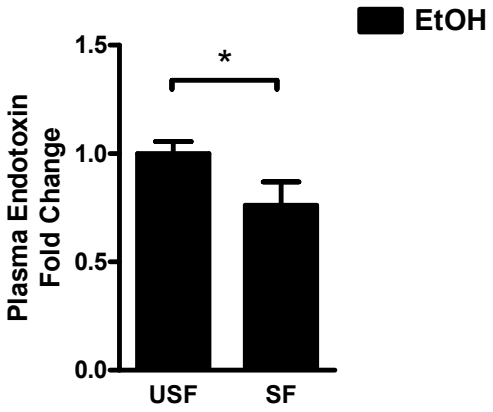

Supplemental Figure 12

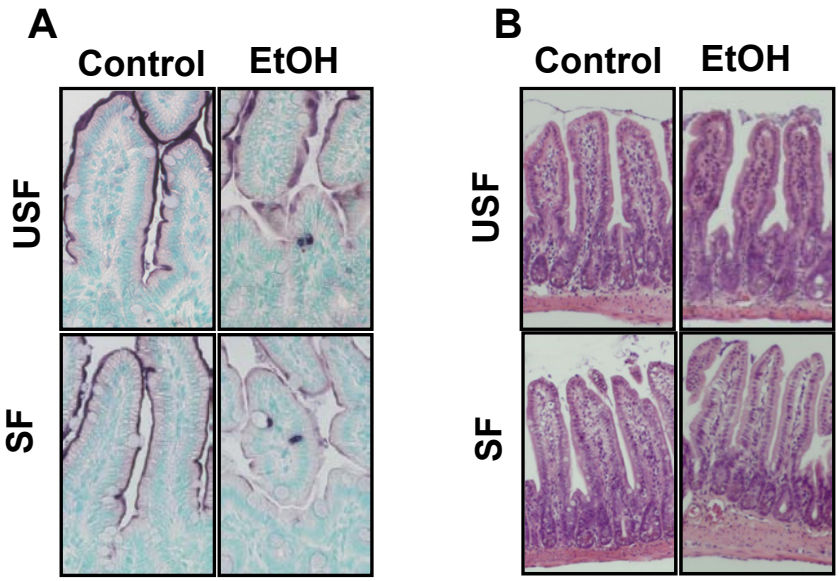

Supplemental Figure 13

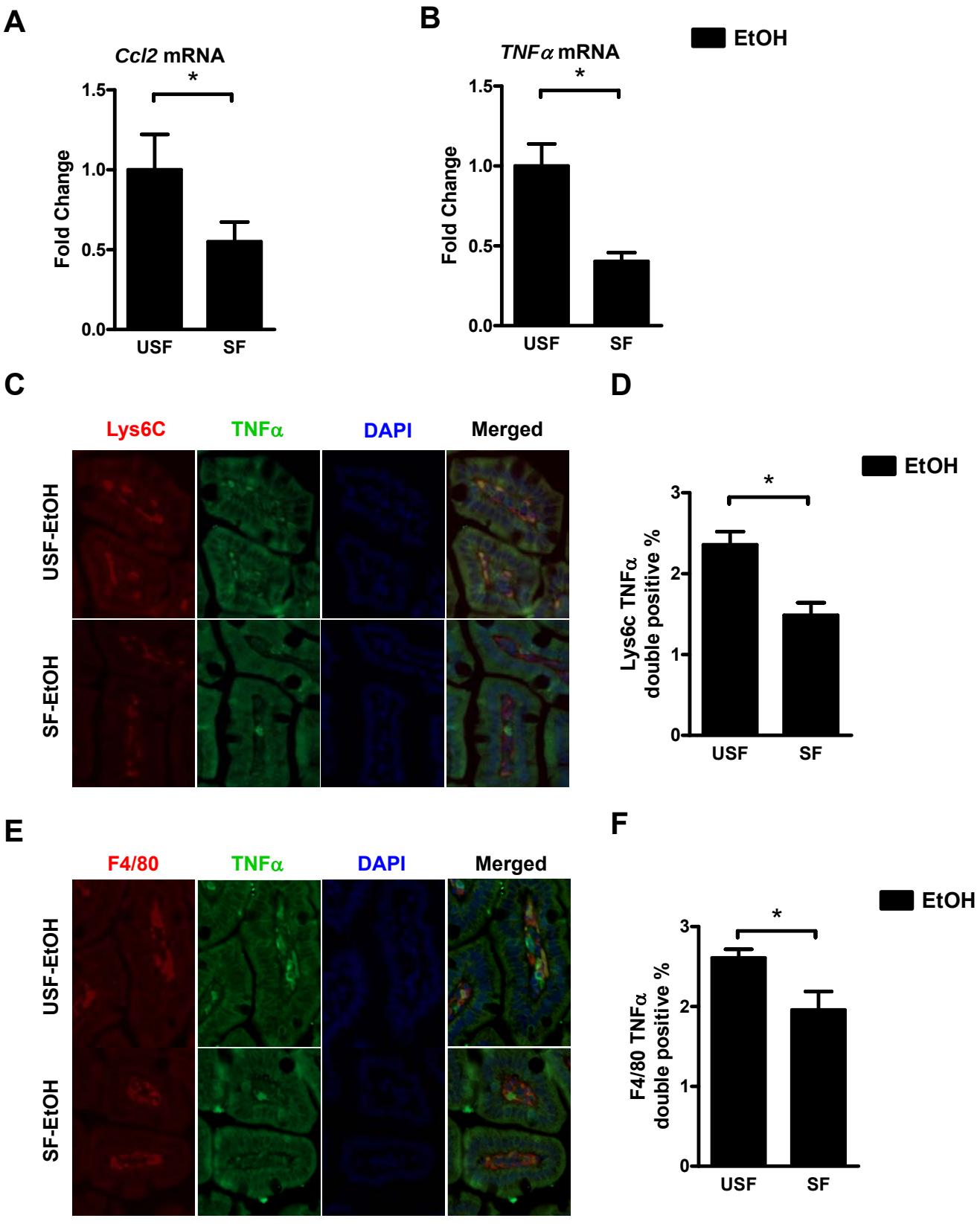

Supplemental Figure 14

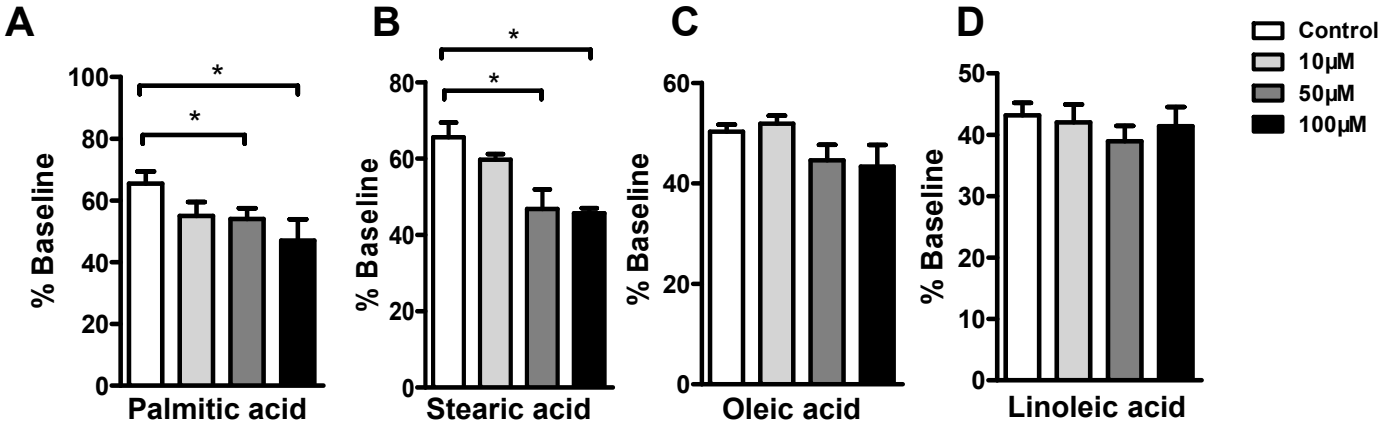

Supplemental Figure 15

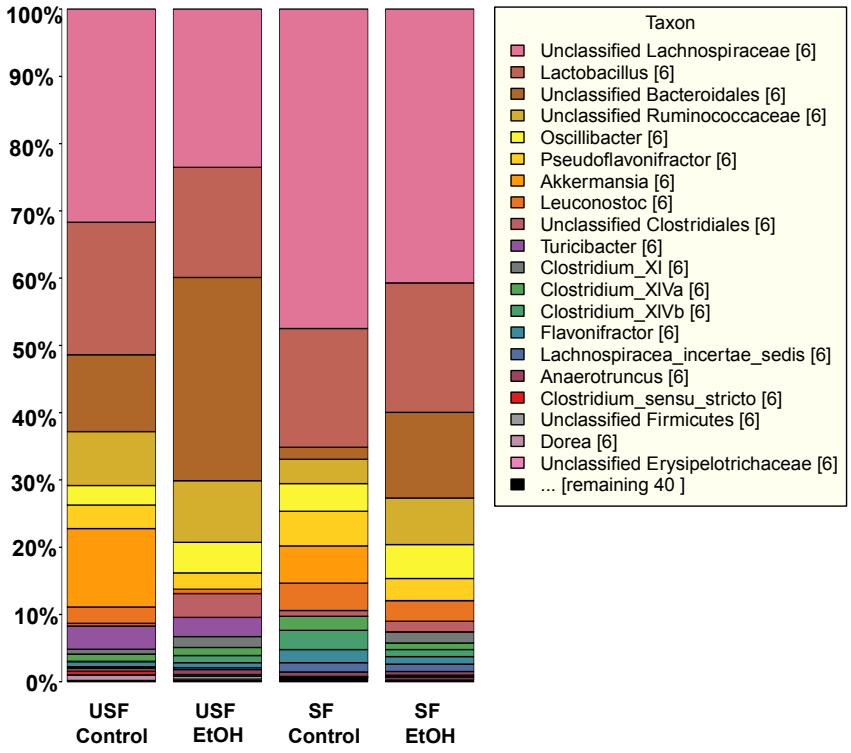

Supplemental Figure 16